Evaluation of Three Ultrasonic Instruments for Critical Velocity Determination during Hanford Tank Waste Transfer Operations - 11121

Jagan Bontha, Kayte Denslow, Harold Adkins, Jeromy Jenks, Carolyn Burns, Phil Schonewill, Gerry Morgen, Margaret Greenwood, Theodore Wooley*

Pacific Northwest National Laboratory, PO Box 999, Richland, Washington 99352
*Washington River Protection Solutions, 639 Cullum Street, Richland, Washington 99354

ABSTRACT

Three ultrasonic instruments were evaluated by the Pacific Northwest National Laboratory (PNNL) to determine their ability to detect critical velocities for solids settling during slurry transfer operation between the Hanford tank farms and the Waste Treatment and Immobilization Plant (WTP). The evaluation was conducted in a flow loop using prototypic transfer piping and a suite of simulants that encompass a broad range of waste physical and rheological properties that will likely be encountered during Hanford tank waste transfer operations. The results from the evaluation are presented in this paper.

INTRODUCTION

The U.S. Department of Energy-Office of River Protection's Hanford Tank Waste Treatment and Immobilization Plant (WTP) is being designed and built to treat and vitrify highly radioactive components of wastes contained in Hanford's 177 underground storage tanks. Delivery of Hanford tank waste to WTP is governed by specific Waste Acceptance Criteria (WAC) that must be certified before any waste can be transferred. ICD 19 - Interface Control Document for Waste Feed identifies the WTP WAC [1]. Critical velocity for solids settling is a key waste acceptance parameter that falls into this category.

Critical velocity during slurry transfer operations is the minimum velocity below which solids settle to the bottom of a horizontal transfer line. Numerous correlations for determining critical velocities of particulate slurries flowing in pipelines exist in the literature. Liddell and Burnett [2] conducted an extensive review of the published critical velocity correlations and concluded that the correlations by Oroskar and Turian [3] and Gillies and Shook [4] are the best candidates for the design of slurry transfer systems at Hanford. However, application of these correlations requires extensive physical and rheological characterization of the waste streams. In addition, Poloski et al. [5, 6] conducted an extensive experimental investigation on pipeline plugging during waste transfers at WTP and concluded that in several situations these correlations under-predict the critical velocities.

The current strategy of Washington River Protection Solutions (WRPS)[1] involves blending waste from different tanks to achieve the targeted properties for delivery to the WTP. Upon blending, the waste circulates through a waste certification loop (see Figure 1) instrumented to allow real-time measurement of the critical velocity and sample collection for feed characterization. The composition of the feed in the blend tank is adjusted until the feed meets the WAC for transfer to the WTP.

---

(1) WRPS is the current US Department of Energy contractor for Hanford tank farm operations.

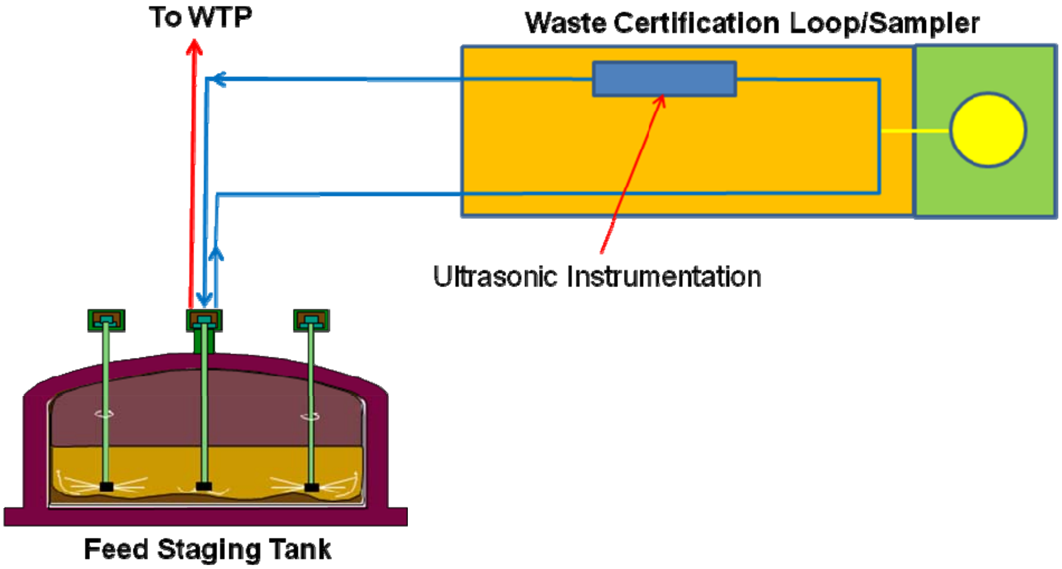

Figure 1. Strategy for Hanford Waste Feed Certification

In 2009, researchers at PNNL conducted an extensive review and assessment of currently available instruments and sensors and selected three ultrasonic instruments – PulseEcho, Ultrasonic Attenuation, and Ultrasonic Doppler Velocimeter – as the most promising candidates for detecting critical velocity and settled bed formation in the field-deployed waste certification loop [7]. Subsequently, in 2010, PNNL evaluated the reliability of the chosen instruments to detect critical velocity using a flow loop consisting of prototypic piping [8, 9]. Presented in the following sections is a description of the ultrasonic instruments, flow-loop, experimental approach, simulants used, data analysis, and results from the evaluation of the three sensors.

ULTRASONIC INSTRUMENTS FOR CRITICAL VELOCITY MEASUREMENT

The three PNNL-developed instruments evaluated in the present study – PulseEcho, Ultrasonic Doppler Velocimeter, and Ultrasonic Attenuation – were identified after a detailed study of the available instruments, their suitability for use during Hanford waste transfer operations, and technology maturity [7]. Presented below is a brief description of the principle behind these instruments. Bontha et al. [8, 9] presents additional information on the three instruments.

The ultrasonic PulseEcho system developed at PNNL addresses the challenges faced by conventional pulse-echo measurement methods during dynamic sediment detection and monitoring. The PNNL-developed PulseEcho system uses a single-transducer in pulse-echo measurement mode. However, the system does not require coherent signal returns in the form of echo patterns to detect and measure interfaces. Rather than relying on coherent echo returns to detect interfaces, the PulseEcho system relies on obtaining incoherent ultrasonic backscatter from an ensemble of sound-scattering particles. Ultrasonic backscatter is the portion of sound energy returned to the transducer after being scattered by the particles (see Figure 2). For backscattering to occur in a fluid, the fluid must contain materials (e.g., particles or "scatterers") that have acoustic impedances that are different from that of the surrounding fluid, and the wavelength of ultrasonic energy in the fluid mixture should be on the same order as the sound-scattering material. A minimum particle inventory must also exist in the sound field or insonified fluid volume to generate sufficient backscatter for a reliable measurement. The minimum number of required particles is dependent on the ultrasonic energy wavelength, the size of the sound field, and the size of the particles. When a sound field produced by an ultrasonic transducer of appropriate frequency interacts with a fluid that contains an ensemble of scatterers, backscattering occurs and manifests as amplitude-modulated signals in the time domain of real-time ultrasonic signals. PNNL's PulseEcho system uses the ultrasonic backscatter in the time domain to identify interfaces between non-moving and moving particles. Moving particles result in an amplitude modulated ultrasonic signal, whereas stationary particles result in a non-modulated signal. The point in time where non-modulated backscatter meets modulated backscatter defines the interface between non-moving and moving particles.

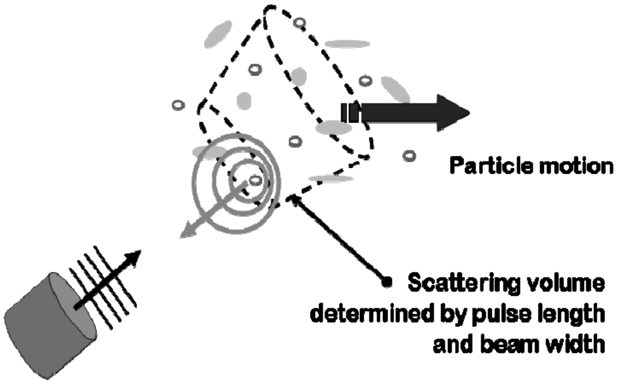

Figure 2. Detecting Particle Motion Using PulseEcho.

Ultrasonic Doppler Velocimetry (UDV) provides a method to make non-disruptive velocity profile measurements of a fluid or slurry flowing in a pipe. This velocity can yield information regarding the formation of a settled bed at the bottom of transfer lines. The ultrasonic Doppler-based system operates by generating a tone burst, which is a specific number of cycles of a sinusoidal waveform at a specific repetition rate. The frequency of the sinusoidal waveform used is largely dependent on the material properties of the test medium and the intended application. Typical applications generally fall in the range from 200 kilohertz (kHz) to 10 megahertz (MHz).

The two main factors that usually determine the frequency of operation are the attenuation of the fluid versus frequency and the sizes of scattering particles in the fluid. In UDV, a tone burst signal applied to an ultrasonic transducer converts the electronic signal into an ultrasound wave and transmitted into the flowing slurry. After transmitting the tone burst ultrasound into the fluid, the same transducer receives the ultrasound echoes from the scattering particles in the fluid. The transducer converts the ultrasound echoes into an electronic signal amplified and processed to extract the Doppler frequency shift. The Doppler frequency shift is correlated to the velocity of the particles in the pipe. Figure 3 depicts a typical cross-sectional view of an ultrasonic transducer mounted in a pipe.

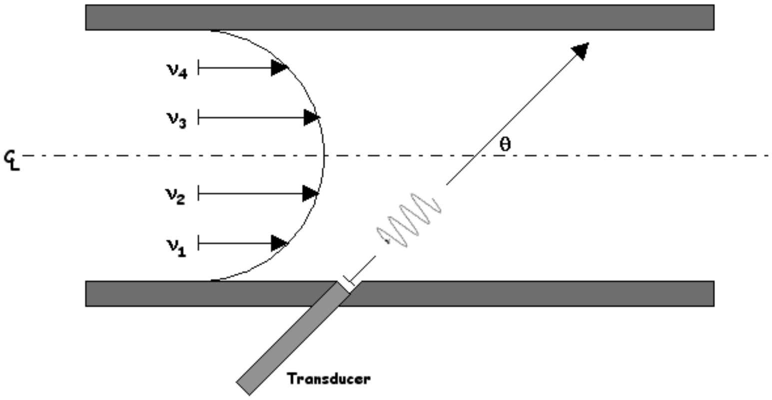

Figure 3. Particle Velocity Measurement Using UDV.

The ultrasonic attenuation system operates by measuring the attenuation of an ultrasonic pulse between a transmit transducer and a receive transducer after the pulse has traveled through a liquid or slurry (Figure 4). As ultrasound travels through a slurry, its signal amplitude is attenuated based on interactions with particles in the slurry, and the receive transducer measures the resultant smaller voltage. Thus, there is a direct correspondence between the attenuation of the ultrasonic pulse and the concentration of the slurry. The attenuation is also dependent on the type and size of the particulate. Qualitative measurements of attenuation in a slurry can be made to monitor trends and infer changes in the slurry. To quantify particle concentration, laboratory measurements are required to develop calibration curves to relate the measured attenuation to particle concentration. For qualitative or quantitative measurements, the attenuation is determined by comparing the attenuation for a given slurry simulant with the baseline attenuation of the carrier liquid (e.g., water).

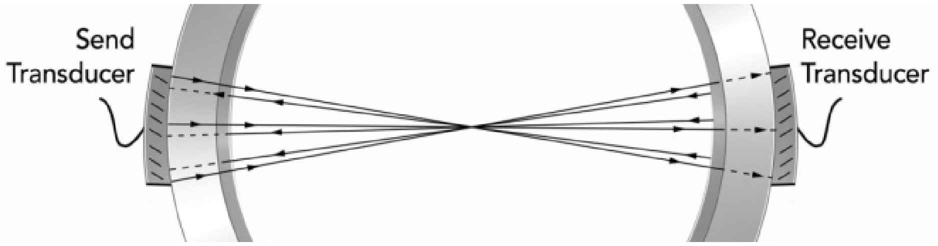

Figure 4. Schematic Diagram of the Ultrasonic Attenuation Sensor.

FLOW LOOP

The flow loop, shown in Figure 5, is composed of various segments of stainless steel pipe and hose, a slurry pump, heat exchanger, loop pressurization system, simulant loading hopper, flush system, video camera, various pressure transducers and thermocouples, a flow meter and the test section containing the evaluated sensors.

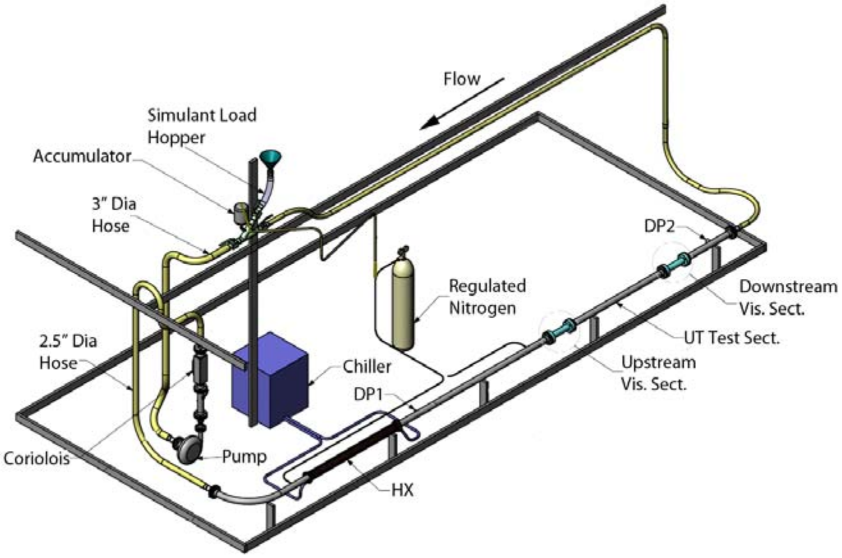

Figure 5. Schematic of the Flow Loop Used to Evaluate the Ultrasonic Sensors

The piping used for the flow loop consisted of horizontal 0.076 m (3 in.), schedule 40 stainless steel sections connected using 0.06 m (2.35 in.) internal diameter flexible hosing to complete the recirculation loop. This ensured that solids settling occurred in the 0.076 m (3 in.) section only and thus was observed by the instruments. A multi-tube-against-pipe heat exchanger was used to reject slurry pump mechanical heating. The loop was designed to be pressurized to 5.4 atm (80 psig) through a 0.019 m^3 (5 gallon) accumulator positioned at the highest point of the loop. Pressurization of the loop minimizes the presence of gas bubbles in the transfer line and improves Coriolis flow meter performance. The slurry was recirculated through the loop using a Georgia Iron Works pump capable of developing average line velocities up to 3.05 m/s (10 ft/s or 230 gpm) and handling fluids ranging from water to a Bingham plastic fluid with a consistency of 30 mPa.s and a yield stress of 30 Pa. A closed-circuit feedback loop from the Coriolis meter mounted upstream of the pump was used in-conjunction with a Hitachi VF-S11 variable frequency drive to maintain a constant flow rate through the loop.

Test Section

The test section consists of an instrumentation spool piece containing the three PNNL-developed instruments. In addition, the test section contained reference instruments and visualization sections that enabled independent determination of the critical velocity for direct comparison with the ultrasonic instruments.

Details of Ultrasonic Instrument Installation

The Pulse Echo transducers were installed on the flattened portion underside of the ultrasonic spool piece (Figure 6). The transducers were 5 MHz, 0.006 m (0.25 in). diameter piezo-composite transducer purchased from NDT Systems, Inc. (Huntington Beach, CA). The wall thickness at the flattened section where the PulseEcho transducer was mounted corresponds to 6×10^{-3} m (0.1 in).

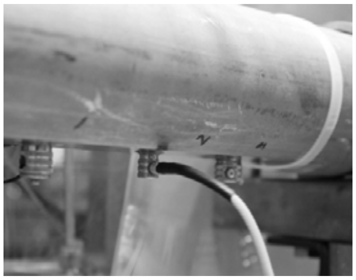

Figure 6. PulseEcho Transducer Mounted on the Instrument Spool Piece

The UDV system does not work well when operating through a stainless steel pipe wall. Therefore, plastic lens with good ultrasonic properties and made out of material suitable for use in a radiation environment (Rexolite®, a crosslinked polystyrene with divinylbenzene, and PEEK, polyetheretherketone) was used as an interface between the ultrasonic transducer (1 MHz) and the fluid as shown in Figure 7.

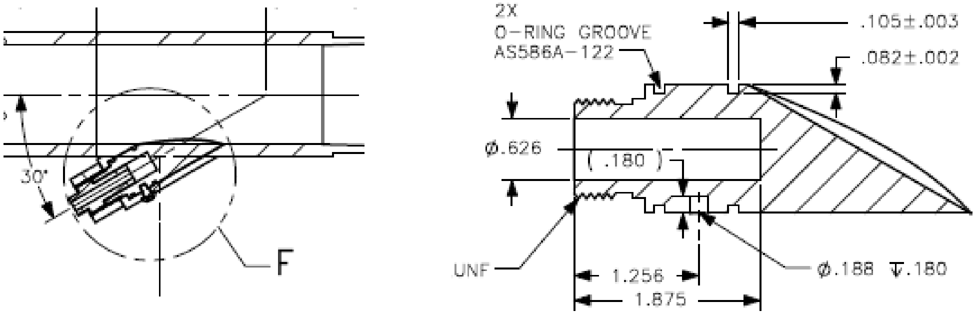

Figure 7. UDV Mounting and Sleeve Assembly

The ultrasonic attenuation (UA) system consisted of a set of three send-receive pairs of 3.5 MHz(2) curved transducers that were fabricated to match the outer diameter of the instrumentation spool piece. The transducers were mounted on the pipe wall in the vertical, horizontal, and 32° angled (from vertical) orientation as shown in Figure 8.

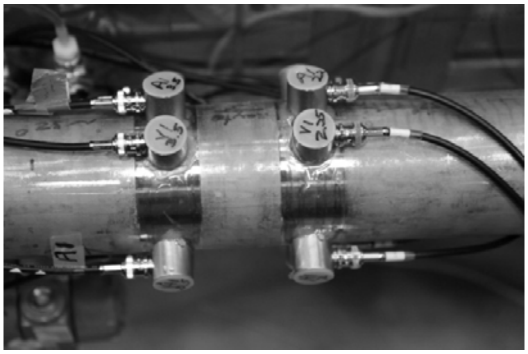

Figure 8. Ultrasonic Attenuation Sensors Mounted on Spool Piece.

---

(2) A second set of six 2.25 MHz transducers were also mounted on the spool piece but data from these transducers was not used in determining the ability of the ultrasonic attenuation system to detect critical velocity.

Reference Instruments

The reference instruments used included differential pressure gauges, transparent visualization sections on both ends of the ultrasonic instrument spool piece, and a video camera mounted on the upstream visualization section to allow focused visual observation of the flow. The differential-pressure transducers used were Rosemount model 1151 with an operating range of 0 to 0.4 atm (0 to 150 in. of H_2O). The pressure transducers, mounted between ports DP1 and DP2 in Figure 5, were connected to the flow loop through open horizontal weldolet connectors. The video camera was a Grasshopper®, Model GRAS-20S4M/C and mounted at the bottom of the upstream visualization section.

Differential pressure transducers are located upstream and downstream of the test section. The distance between port legs (DP1 and DP2) is 5.7 m (18.75 ft). DP1 and DP2 are located at least 40 pipe diameters after and 5 pipe diameters prior to any potential flow disturbance such as elbows and welds protrusions. The UT test section was located at least 73 diameters from flow disturbances. Complete detailed drawings of the loop and the ultrasonic instrument test section can be found in Bontha et al. [8, 9].

SIMULANTS

A matrix of 25 tests was formulated to evaluate the performance of the three sensor technologies. Each test had a unique particle system and carrier fluid combination. Particle systems ranged from single-component systems with a narrow particle size distribution (PSD) to multi-component systems with a broad range of particle sizes. Carrier fluids span Newtonian and non-Newtonian rheologies (including carrier fluids with a finite yield stress). The physical property ranges examined during the testing are listed in Table 1.

Table 1. Properties of Simulants Used during Testing.

Physical Property	**Tested Range**
Particle Size	~7 to 600 µm
Particles Type and Particle Densities	Glass (2500 kg/m^3), High Density Glass (4180 kg/m^3), Aluminum Hydroxide (2420 kg/m^3), Alumina (3770 kg/m^3), Zirconium Hydroxide (2500 kg/m^3)
Weight Percent Solids	5, 10, and 20%
Carrier Fluids and Densities	Water (1000 kg/m^3), Water/Glycerin (1150 kg/m^3); Kaolin/water (1250 kg/m^3)
Newtonian Simulants	Water – 1 mPa.s; Water/Glycerin – 11.7 mPa.s
Non-Newtonian Simulants	Kaolin/water mixtures: Bingham yield stress – 1.9 to 10.5 Pa; Bingham Consistency – 2.3 to 7.9 mPa.s

TEST APPROACH

The same test procedure was followed for all of the tests conducted. At the start of a test evolution, the flow loop was empty. The loop was first configured for loading the simulant. Simulant loading involved adding pre-weighed solids through the hopper either as slurry or as dry powder. After all solids were added, the loop was filled with the carrier fluid until all air had been expelled from the system. The loop was then closed and pressurized to 5.4 atm (80 psig).

To begin a test, the pump was initially operated at a high flow velocity (typically around 2.4 m/s or 8 ft/s) to mobilize and suspend the particles. The test proceeded by setting the flow velocity and giving the system time to reach steady state before the ultrasonic instruments collected data. Steady state was determined from visual observations and real-time analysis of the Coriolis and differential pressure data. Steady state was usually observed 7 to 15 minutes from the time the velocity was set; however, there were some instances when it took an hour or more.

The flow velocity set points began at 2.4 m/s (8 ft/s) and decreased by 0.3 m/s (1 ft/s) until critical velocity (i.e., a stationary bed) was surpassed. The slurry was brought back up to a high velocity (typically 2.4 m/s or 8 ft/s) to resuspend the particles. After resuspension, the velocity was reduced in smaller increments to set points near the region where a settled bed was first observed to determine the critical velocity within ±0.03 to 0.06 m/s (±0.1 to 0.2 ft/s). At each velocity step, data was gathered with each ultrasonic sensor and visual observations were made to characterize the flow behavior and identify the formation of a stationary bed. The data collection portion of the test was complete once the differential pressure data was verified to match the data from the start of the test. The only deviations from this procedure for non-Newtonian simulants included shearing the slurry in the loop at a high velocity for ~1 hour and collection of a sample for rheology characterization after shearing at the start and end of the test.

DATA ANALYSIS

Experimental Critical Velocity Observations

In general, three distinct flow regimes were observed immediately preceding the formation of a stationary bed of particles. These included: Regime I consisting of focused circumferential chaotic particle motion, Regime II consisting of focused axial motion or a sliding bed, and Regime III consisting of pulsatory (stop/go) sliding bed. The regimes are illustrated in Figure 9.

Of the three regimes discussed above, Regimes II and III were taken as indications that the particles were on the verge of settling out.

PulseEcho Data Analysis

The ultrasonic PulseEcho system detects the onset of solids settling by detecting the presence or lack of ultrasonic backscatter from particles in a process stream near the pipe wall. The particle composition, size and concentration will contribute to the acoustic scattering efficiency, or strength. If signal modulation from the process stream particles coincides with the t = 0 μs pipe wall signal in the time-based ultrasonic signal, then all particles at and beyond the pipe wall are considered mobilized and no sediment is reported. However, if modulation does not coincide with the reference pipe wall signal, and instead occurs beyond this point in time, the modulation time value is measured and subsequently used to calculate a sediment depth.

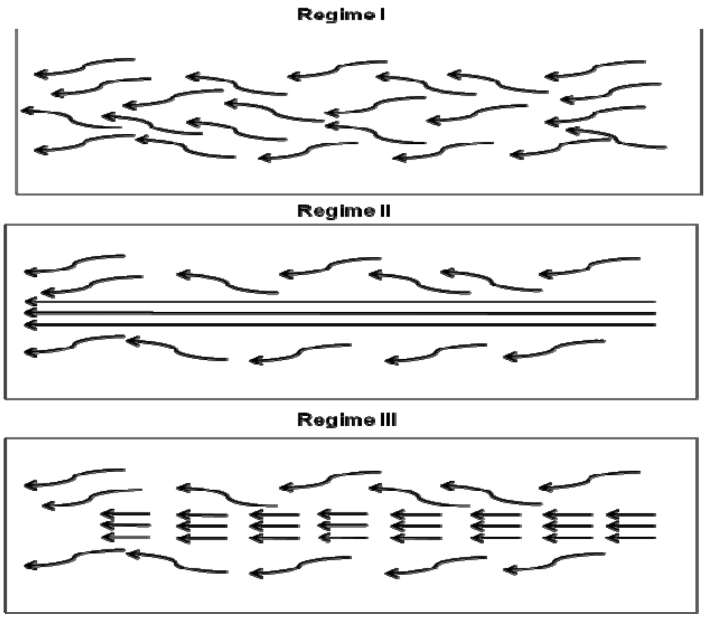

Figure 9. Regimes Preceding the Critical Velocity: Regime I - Focused Circumferential Chaotic Motion, Regime II - Focused Axial Motion (Sliding Bed), Regime III - Pulsatory (Stop/Go) Sliding Bed. View is from the Bottom of the Visualization Section.

Indications of settling are reported when signal modulation crossed the PulseEcho algorithm variance threshold. Since intermittent solids settling can occur near the critical velocity, the reported flow velocities at which the PulseEcho system detected solids deposition represent those where at least 10% of the measured sediment depth values were greater than zero over the 1 to 2 minute measurement period. Figure 10 presents an example illustrating critical velocity determination with PulseEcho. In this figure, the horizontal axis represents the sequence of flow velocities studied during the test as discussed in the Test Approach section above. The vertical axis represents the percentage of critical settling velocity indications reported by PulseEcho during the 1 to 2 minute measurement period for each flow velocity evaluated. It can be seen from Figure 10 that as the velocity was reduced from 2.4 m/s (8 ft/s) to 0.9 m/s (3 ft/s), first indications of a settled bed formation (i.e., the measured indications from the PulseEcho signal was greater than the 10% threshold shown by the horizontal line) was noted at 1.22 m/s (4 ft/s). However, during fine tuning of the critical velocity determination between 1.34 to 1.19 m/s (4.4 to 3.9 ft/s), the >10% threshold indication for a settled bed formation occurred at 1.19 m/s (3.9 ft/s) and this value was recorded as the measured critical velocity using PulseEcho.

UDV Data Analysis

In general, a close examination of the UDV data collected during the present testing campaign indicated that at velocities greater than the critical velocity, the measured UDV profiles in the pipe section rapidly increase from the pipe wall to a peak value at or near the pipe centerline. As the fluid velocity transitions past critical velocity, the UDV data was marked by the formation of a flat region or a very-low velocity region at the start of the UDV velocity profile plot. This flat or very-low velocity region quickly transitions to higher velocity values, indicating particle movement beyond the flat region.

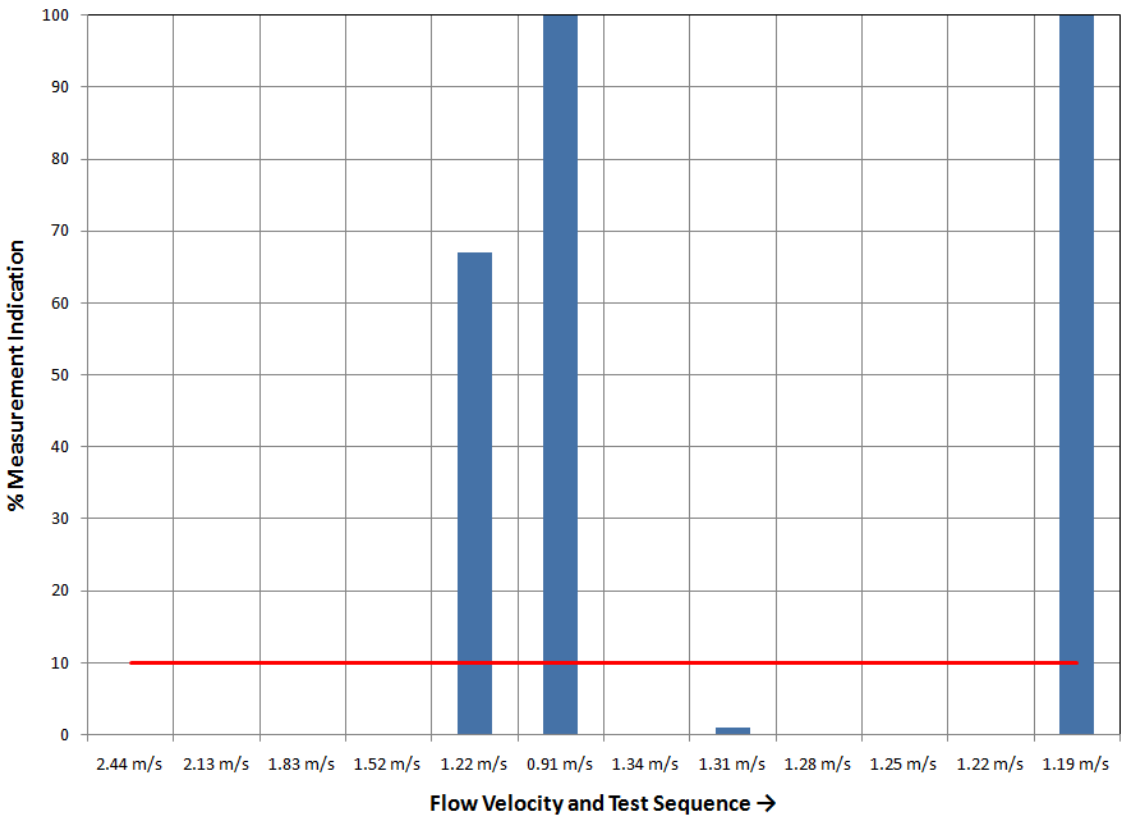

Figure 10. Typical PulseEcho Data for Critical Velocity Determination (Test #6).

In the present analysis, this flat region or very low velocity region was considered as the indication of a settled bed where there is no (or almost no) flow. Hence, this was chosen as the point where the critical velocity was exceeded. This is illustrated in Figure 11. The top curve in this figure represents the coarse critical velocity determination part of the test approach while the bottom curve represents the fine determination of the critical velocity.

It can be seen from the top part of Figure 12, UDV indicates that a stationary bed formation was first detected at 1.22 m/s (4 ft/s) and the thickness of the bed increases as the flow velocity is decreased. Looking at the bottom part of Figure 11, it can be seen that the bed formation begins at 1.25 m/s (4.1 ft/s) and this value was recorded as the measured critical velocity using by UDV.

Note - It can also be seen from these two plots that the velocity value that indicates a settled bed is not zero, but on the order of 0.095 m/s (0.3 ft/s). This small offset value for an indication of a settled bed is an artifact of the data analysis algorithm used in this version of UDV to identify the Doppler frequency shift at a range increment.

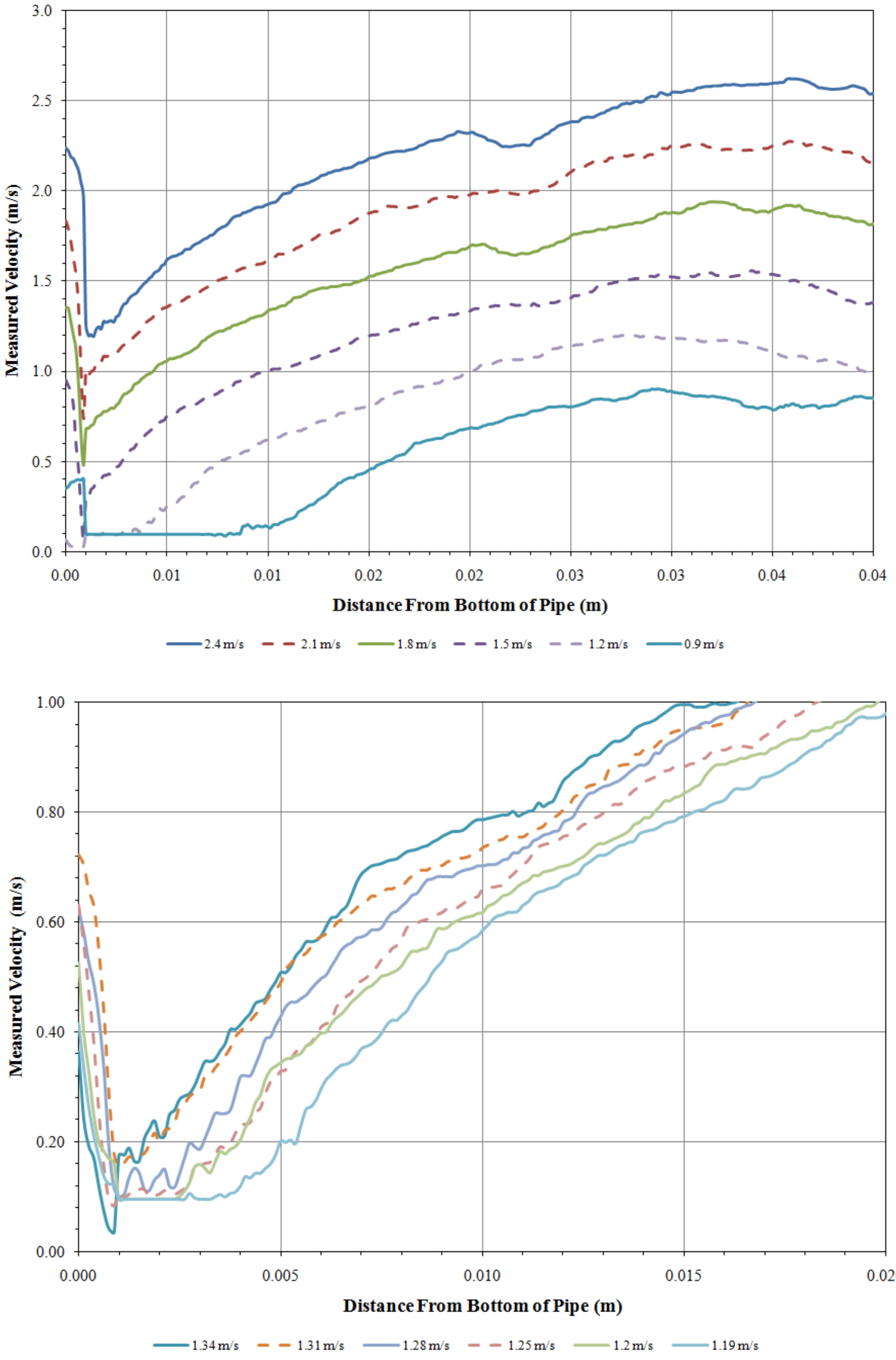

Figure 11. Typical UDV Data for Critical Velocity Determination (Test #6). Top – Coarse Critical Velocity Determination Step; Bottom – Fine Critical Velocity Determination Step.

Ultrasonic Attenuation Data Analysis

A close examination of the UA data indicated that the critical velocity can be inferred from trends in the ratio of the voltage measured by the vertically mounted transducer after ultrasound travels through the slurry (V_s) to the voltage measured by the same transducer in water (V_w). In most cases, when the slurry was moving at or near critical velocity, the standard deviation in the ratio V_s/V_w increased significantly compared to its value at very high slurry velocities (e.g., 2.4 m/s or 8 ft/s). Although the reason for the observed behavior is not currently understood, the maximum or minimum in the standard deviation of V_s/V_w was used to determine the critical velocity. This is illustrated in Figure 12. The data in this figure shows that the normalized standard deviation exhibits a maximum at 1.25 m/s (4.1) ft/s, and this was recorded as the critical velocity determined by the Ultrasonic Attenuation system.

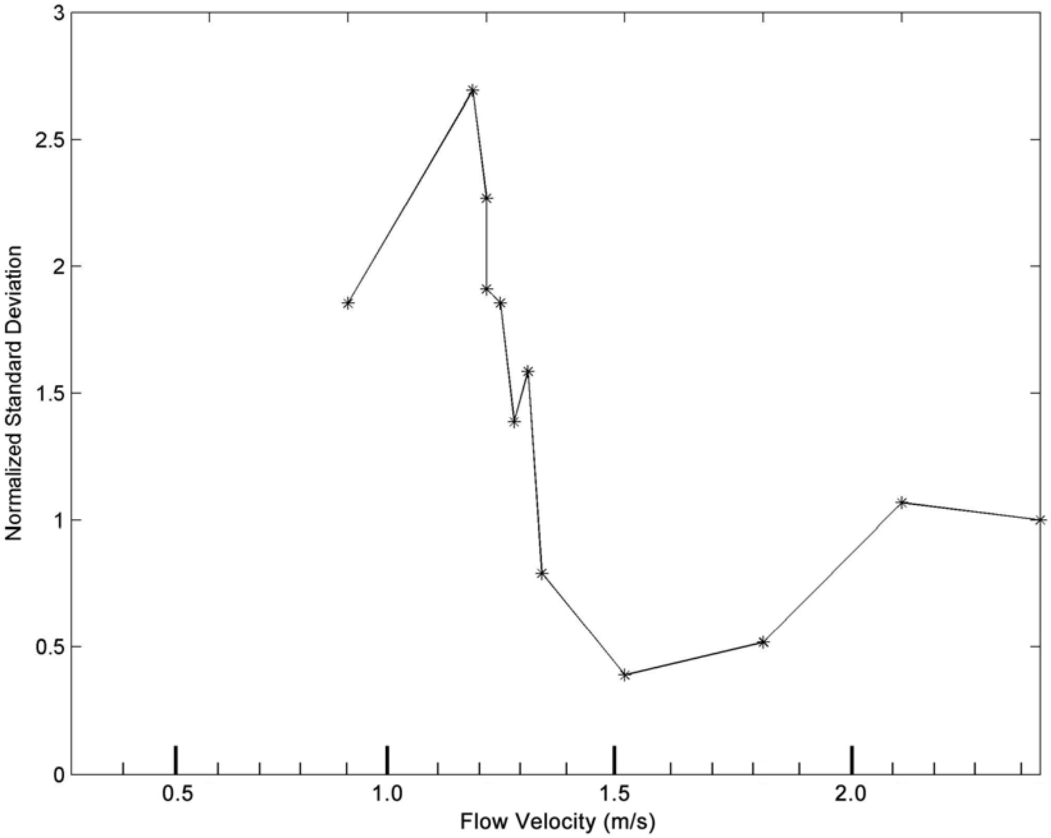

Figure 12. Typical UA Data for Critical Velocity Determination (Test #6)

RESULTS AND DISCUSSION

Table 2 presents an overview of the critical velocities for all the Newtonian simulant tests as measured by the three ultrasonic instruments along with the experimentally measured critical velocities. The data for the non-Newtonian simulants is shown in Table 3. Note that on several tests a range was reported for the visual observation for the critical velocity (i.e., stationary bed formation). During these tests, a stationary bed did not form at the same time in the upstream and downstream visualization sections. Thus, a range was reported that spans the velocity at which the bed first formed in either the upstream or downstream section and the velocity where the bed was observed in both sections. Also included in this table are the velocity information for focused axial motion and a pulsating bed (Regimes II and III as discussed previously); these regimes typically indicate the onset of critical velocity.

Table 2. Critical Velocity Measurements for Newtonian Simulants

Test Number	Simulant Type	Experimental Measurements m/s (ft/s)			Ultrasonic Sensor Measurements m/s (ft/s)		
		R II	**R III**	$V_{critical}$	**PulseEcho**	**UDV**	**Attenuation**(c)
1	Mono-dispersed (s1-d2)	**n/a**	**n/a**	**0.73 (2.4)**	**0.73 (2.4)**	**0.73 (2.4)**	N/A
2	Mono-dispersed (s1-d2)	**0.84 (2.75)**	**0.81 (2.65)**	**0.78 (2.55)**	**0.81 (2.65)**	**0.81 (2.65)**	N/A
3	Mono-dispersed (s2-d2)	**1.34 (4.4)**	**1.31 (4.3)**	**1.28 (4.2)**	**1.25 (4.1)**	**1.31 (4.3)**	**1.52 (5.0)**
4	Broad PSD	**1.10 (3.6)**	**1.07 (3.5)**	**1.01 (3.3)**	**1.01 (3.3)**	**1.01 (3.3)**	**1.37 (4.5)**
5	Broad PSD	**1.28 (4.2)**	**1.25 (4.1)**	**1.22 (4.0)**	**1.22 (4.0)**	**1.25 (4.1)**	**1.28 (4.2)**
6	Mono-dispersed (s1-d1)	**1.28 (4.2)**	**1.25 (4.1)**	**1.19 (3.9)**	**1.19 (3.9)**	**1.25 (4.1)**	**1.25 (4.1)**
7	Mono-dispersed (s1-d1)	**0.88 (2.9)**	**0.85 (2.8)**	**0.76 (2.7)**	**0.88 (2.9)**	**0.76 (2.8)**	**0.73 (2.4)**
8	Mono-dispersed (s1-d4)	**0.75 (2.45)**	**--**	**0.72 (2.35)**	**0.72 (2.35)**	**0.72 (2.35)**	**0.64 (2.1)**
9	Binary size (s1-d1(33%)/s1-d2 (67%))	**1.00 (3.3)**	**0.97 (3.2)**	**0.95 (3.1)**	**1.04 (3.4)**	**0.91 (3.0)**	**0.91 (3.0)**
10	Binary size (s1-d1 (67%)/s1-d2 (33%))	**1.28 (4.2)**	**>1.25 (4.1)**	**1.25 (4.1)**	**1.37 (4.5)**	**1.25 (4.1)**	**1.25 (4.1)**
11	Binary density (s1-d2 (67%)/s2-d2 (33%))	**1.22 (4.0)**	**1.20 (3.9)**	**1.16 (3.8)**	**1.25 (4.1)**	**1.16 (3.8)**	**1.10 (3.6)**
12	Broad PSD	**~0.91 (3.0)**	**0.85 (2.8)**	**0.82 (2.7)**	**~0.79 ~(2.6)**	**>0.69& < 0.76 (>2 & <2.5)**	**0.79 (2.6)**
13	Bi density Broad PSD	**1.49 (4.9)**	**1.33 (4.7)**	**1.40 (4.6)**	**1.49 (4.9)**	**>1.22 & <1.40 (>4.0 & <4.6)**	**1.31 (4.3)**
25	Broad PSD	**1.28 (4.2)**	**1.22 (4.0)**	**1.12 (3.7)**	**1.22 (4.0)**	**1.16 – 1.19 (3.8 – 3.9)**	N/A

(a). R II and R III correspond to flow velocities where focused axial motion or a pulsating (stop/go) bed, respectively, was observed at the bottom of the pipe is moving. $V_{critical}$ corresponds to the velocity at which a stationary bed was observed.

(b). N/A = No data available

(c). An average value is shown for situations where multiple indications were possible for the attenuation system.

(d). 60 wt% glycerin, Newtonian viscosity 11.7 mPa.S

🟩	Sensor measurement sensor falls within the range for R II, RIII, and $V_{critical}$
🟧	Sensor measurement sensor falls **within ±0.3 ft/s** of the range for R II, RIII, and $V_{critical}$
🟥	Sensor measurement sensor falls **outside ±0.3 ft/s** of the range for R II, RIII, and $V_{critical}$

Table 3. Critical Velocity Measurements for Non-Newtonian Simulants.

Test #	**Simulant Type**	**Yield Stress (Pa)**	**Exp. Measurements m/s (ft/s)**[a,b]			**Ultrasonic Sensor Measurements m/s (ft/s)**		
			R II	**R III**	**$V_{critical}$**	**PulseEcho**	**UDV**	**Attenuation**[c]
14	Carrier fluid-Koalin	8.2	--	--	--	--	--	--
15	Mono-dispersed (Mil#8)	10.5	--	--	**0.64-0.70 (2.1-2.3)**	**0.64 (2.1)**	**0.64 (2.1)**	N/A
16	Mono-dispersed (Mil#8)	8.8	**1.22 (4.0)**	**0.97 (3.2)**	**0.79-0.91 (2.6-3.0)**	**0.95 (3.1)**	**0.97 (3.2)**	N/A
17	Broad PSD	8.5	**1.28 (4.2)**	--	**1.10 (3.6)**	**1.16 (3.8)**	**1.10 (3.6)**	**1.28 (4.2)**
18	Broad PSD	3.4	**1.16 (3.5)**	**0.95 (3.1)**	**0.91 (3.0)**	**0.95 (3.1)**	**0.91 (3.0)**	**0.85 (2.8)**
19	Mono-dispersed (Mil#13)	10.4	--	**0.09 (0.3)**	**0.06 (0.2)**	**0.15 (0.5)**	**0.30 (1.0)**	**0.12 (0.4)**
20	Mono-dispersed (Mil#13)	11.35	--	**0.43 (1.4)**	**<0.30 (<1.0)**	**0.45 (1.5)**	**0.45 (1.5)**	**0.36 (1.2)**
21	Duralum-Broad PSD	1.9	**0.97 (3.5)**	**1.04 (3.4)**	**0.95-1.01 (3.1-3.3)**	**0.95 (3.1)**	**0.95 - 0.98 (3.1 - 3.2)**	**0.85 (2.8)**
22	Complex simulant	2.3	**1.07 (3.3)**	**1.04 (3.4)**	**0.95-1.01 (3.1-3.3)**	**1.01 (3.3)**	**1.01 (3.3)**	**1.01 (3.3)**
23	Complex simulant	5.1	**1.31 (4.3)**	**1.28 (4.2)**	**1.1-1.16 (3.6-3.8)**	**1.13 (3.7)**	**1.19 (3.9)**	**1.37 (4.4)**
24	Complex simulant	9.7	**1.52 (5.0)**	**1.28 (4.2)**	**1.25-1.43 (4.1 – 4.7)**	**1.31 (4.3)**	**1.40 (4.6)**	**1.34 (4.4)**

(a). R II and R III correspond to flow velocities where focused axial motion (sliding bed) or a pulsating (stop/go) bed, respectively, was observed at the bottom of the pipe is moving. $V_{critical}$ corresponds to the velocity at which a stationary bed was observed.

(b). N/A = No data available

(c). An average value is shown for situations where multiple indications were possible for the attenuation system.

🟩	Sensor measurement sensor falls within the range for R II, RIII, and $V_{critical}$
🟧	Sensor measurement sensor falls **within ±0.9 m/s (0.3 ft/s)** of the range for R II, RIII, and $V_{critical}$
🟥	Sensor measurement sensor falls **outside ±0.9 m/s (0.3 ft/s)** of the range for R II, RIII, and $V_{critical}$

In Tables 2 and 3, the performance of a sensor is considered excellent when the sensor measurement falls within the experimentally observed range for Regime II, Regime III, and $V_{critical}$. This is shown by shading the cells in "GREEN". On the other hand, if the ultrasonic sensor measurement falls within ± 0.09 m/s (0.3 ft/s) of this range, the sensor performance was still considered good and indicated by shading the cells in "AMBER". Finally, if an ultrasonic measurement falls outside this range, the sensor performance was considered poor and indicated by shading the cells in "RED". A GREEN/AMBER/RED shading of the cells provides a quick assessment of the sensor performance.

The data in Tables 2 and 3 show that both the PulseEcho and the UDV systems are in excellent agreement with the experimentally observed critical velocities. Also, for the tests where the PulseEcho or UDV measurements are designated "AMBER" or "RED", either the errors are small or the critical velocity occurred at a velocity that is far below a velocity that would be of concern during slurry transfer operations (i.e., << 0.3 m/s or 1 ft/s).

CONCLUSIONS

Three PNNL-developed ultrasonic sensors – Pulse Echo, Ultrasonic Doppler Velocimetry, and Ultrasonic Attenuation – were evaluated for their ability to detect critical velocity during slurry transfer operations at Hanford. Over the range of simulants evaluated, both PulseEcho and UDV performed exceptionally well in detecting critical velocities. Based on the observed performance of the sensors, both PulseEcho and UDV are considered excellent candidates for use in the waste certification loop.

REFERENCES

1. Hall MN. 2008. ICD-19 – Interface Control Document for Waste Feed. 24590-WTP-RPT-PE-07-001. Bechtel National, Inc. Richland, WA.

2. Lidell KC and DF Burnett. 2000. Critical Transport Velocity: A Review of Correlations and Models. RPP-7185, Rev. 0, CH2M Hill Hanford Group, Richland, WA.

3. Oroskar AR and RM Turian. 1980. The Critical Velocity in Pipeline Flow of Slurries. *AICHE Journal* 26(4), 550-558.

4. Gillies, RG and CA Shook. 1991. A Deposition Velocity Correlation for Water Slurries. *Canadian Journal of Chemical Engineering*, 69(5), 1225-1228.

5. Poloski AP, HE Adkins, J Abrefah, AM Casella, R Hohimer, F Nigl, MJ Minette, JJ Toth, JM Tingey, and SM Yokuda. 2009a. Deposition Velocities of Non-Newtonian Slurries in Pipelines. PNNL-17639, WTP-RPT-175 Rev. 0. Pacific Northwest National Laboratory, Richland, WA.

6. Poloski AP, ML Bonebrake, AM Casella, MD Johnson, JJ Toth, HE Adkins, Jr., J Chun, KM Denslow, M Luna, and JM Tingey. 2009b. Deposition Velocities of Non-Newtonian Slurries in Pipelines: Complex Simulant Testing . PNNL-18316, WTP-RPT-189 Rev. 0. Pacific Northwest National Laboratory, Richland, WA.

7. Meyer PA, HE Adkins, KM Denslow, JA Bamberger, BE Wells, MS Greenwood, PA Scott, J Blanchard, GP Morgen. 2009a. Hanford Tank Farms Waste Certification Flow Loop Test Strategy. PNNL-19441, Rev. 0, Pacific Northwest National Laboratory, Richland, WA.

8. Bontha JR, HE Adkins, KM Denslow, JJ Jenks, CA Burns, PP Schonewill, GP Morgen, MS Greenwood, J Blanchard, TJ Peters, PJ MacFarlan, EB Baer, WA Wilcox. 2010. Test Loop Demonstration and Evaluation of Slurry Transfer Line Critical Velocity Measurement Instruments. PNNL-19560, Pacific Northwest National Laboratory, Richland, WA.

9. Bontha JR, HE Adkins, KM Denslow, JJ Jenks, CA Burns, PP Schonewill, GP Morgen, MS Greenwood, J Blanchard, TJ Peters, PJ MacFarlan, EB Baer, WA Wilcox. 2010. Supplementary Information for Test Loop Demonstration and Evaluation of Slurry Transfer Line Critical Velocity Measurement Instruments. PNNL-19560, Pacific Northwest National Laboratory, Richland, WA.